ce/papers Proceedings in civil engineering

Ernst & Sohn A Wiley Brand

Check for updates

ORIGINAL ARTICLE

eurosteel AMSTERDAM 2023

Ernst & Sohn A Wiley Brand

# Experimental and numerical study of a damage-free self-centring link for seismic resilient EBFs

Annarosa Lettieri[1] | Fabio Freddi[2] | Massimo Latour[1]

**Correspondence**

Annarosa Lettieri
Department of Civil Engineering
University of Salerno
Email: alettieri@unisa.it

[1] University of Salerno, Salerno, Italy
[2] University College London, London, UK

**Abstract**

Significant progress has been made in recent years for the definition of seismic-resilient structures, chasing the urgent need for structures able to return to undamaged, fully functional conditions in a short time after an extreme event. Seismic-resilient steel structures have been widely investigated, mainly considering solutions based on moment-resisting and concentrically braced frames. However, while the first category may be characterised by low stiffness, the second is often characterised by low ductility. Eccentrically Braced Frames (EBFs) allow overcoming these drawbacks and well-balance stiffness, strength and ductility. This paper presents the numerical and experimental study of a damage-free self-centring link for EBFs. The proposed device uses post-tensioned bars to control the self-centring behaviour and friction devices to provide dissipation capacity. Experimental cyclic tests have been carried out to evaluate the response of the device. A 3D ABAQUS model has been developed to investigate the local response. Finally, a six-storey EBF has been numerically investigated in OpenSees to evaluate the global response. Incremental Dynamic Analyses were performed demonstrating the increased seismic performance of the proposed solution.

**Keywords**

Seismic resilient, Experimental tests, Steel eccentrically braced frames, Damage-free, Self-centring, Seismic link.

## 1 Introduction

According to current seismic codes (i.e., [1]), Eccentrically Braced Frames (EBFs) are designed to sustain strong earthquakes by promoting the dissipation of the seismic input energy through yielding of the seismic links, which are conventionally made continuous with the collector beams. This codified design approach meets the required safety performance level but implies the development of significant damage and residual deformations, which could limit the repairability of the structures [2]. Innovative systems addressing these drawbacks proposed the use of replaceable links. In these solutions, the seismic links are separate from the non-dissipative elements employing link-beam end-plate or web connections [3],[4], or brace attachments [5]. Nevertheless, although replaceable links allow for isolating the damaged links, the replacement process could be limited by residual deformations (due to the residual misalignment of the links' ends). FEMA P-58 [6] identifies two damage states in terms of residual deformations. Damage State 1 (DS1), with a drift limit of 0.2%, corresponds to damage conditions where structures can be repaired without the need for realignment. Damage State 2 (DS2), with a drift limit of 0.5%, represent the limit over which reparation of the structure is typically not economically convenient, and the option of demolition/reconstruction may be preferred. Similarly to DS2, McCormick *et al.* [7] suggest a permissible residual drift of 0.5% to allow the repairability of the structures.

Self-centring structures have been developed over the year to control structural damage and improve self-centring capabilities [8]-[13]. Self-centring solutions for EBFs have been proposed only recently. Among others, Dubina *et al.* [14] investigated a combination of EBFs with removable links and elastic Moment Resisting Frames (MRFs) to prevent residual deformations. Further studies focused on self-centring systems for EBFs using elastic gap-opening mechanisms at beam-to-link [15] or beam-to-column interfaces [16],[17]. Moreover, other solutions are based on the use of super-elastic shape memory alloy (SMA) elements [18]-[20].

Within this context, the authors have recently proposed a damage-free self-centring link (SC-link) for EBFs [21]. The seismic device, located between the collector beams and connected through pins, employs post-tensioned high-strength steel bars (PT-bars) with disk springs to control the self-centring capacity of the frame and friction devices (FDs) to dissipate seismic energy. The SC-link is composed of a T-plate and two L-plates connected to the top and



https://doi.org/10.1002/cepa.2474

bottom flanges of the beams, as shown in Figure 1. The FDs are made of friction pads, pre-stressed with high-strength bolts, placed at the interface of the T- and L-elements, and realised with slotted holes designed to accommodate the gap opening. The disk springs are arranged in parallel and series to provide sufficient deformability to the connection and an adaptable stiffness-resistance combination.

This paper presents the experimental test's results to characterise the SC-link's cyclic response and verify its self-centring capacity. The SC-link is designed and tested under cyclic loading according to the AISC standardised protocol. 3D Finite Element (FE) models have been developed in ABAQUS [23] and validated against test results to investigate the local response of the device. Moreover, to evaluate the effects of the proposed device on the seismic performance of EBFs, a six-storey case-study structure is designed according to Eurocode 8 and successively upgraded with SC-links. The seismic performances of the EBFs with conventional links (EBF) and with SC-links (SC-EBF) have been investigated and compared by performing Incremental Dynamic Analyses (IDAs) on simplified two-dimensional (2D) models in OpenSees [24].

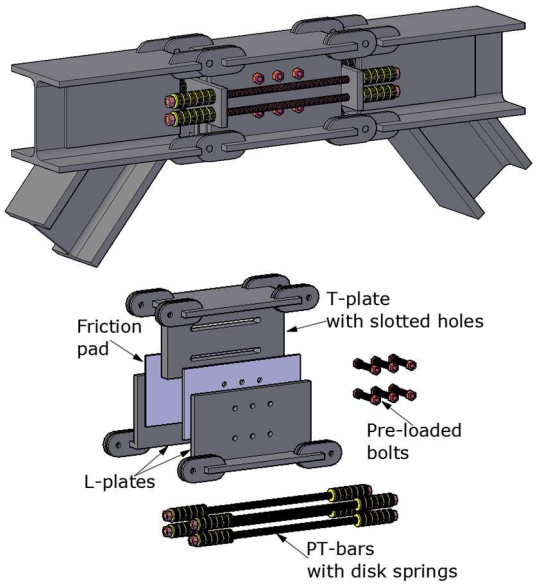


**Figure 1** Proposed damage-free self-centring link for EBFs.

## 2 Damage-free self-centring link

### 2.1 Seismic demand and cyclic behaviour

This section describes the primary assumption and the adopted analytical model to describe the seismic response of the device in terms of forces and displacement/rotation. According to Kasai [25], analytical formulations describing the frame's force-displacement (or moment-rotation) response can be defined considering an EBF sub-assembly hinged at the base. With this simplification, the deformed shape and the free-body diagram of the forces acting on a generic EBF can be represented in Figure 2(a) and (b), respectively, together with the relationship between the deformation parameters and the internal forces acting on the isolated SC-link. Notably, the forces acting along the *x*-direction on the SC-link are longitudinal shear forces ($F_l$), while transverse shear forces (V) act along the *z*-direction. As a result, the expected internal forces can be obtained as follows:

$$\boldsymbol{V = \frac{FH}{L};\quad M = \frac{Ve}{2};\quad F_l = \frac{FHe}{L(h_d - t_f)}} \qquad (1)$$

where $H$ is the storey height; $L$ is the span length; $F$ is the storey's shear force, $e$ is the link's length; $t_f$ and $h_d$ are, respectively, the flange thickness and the section height of the link. Figure 2(c) shows the SC-link's rotation generating the gap-opening mechanism of the connection and the corresponding longitudinal sliding (denoted with $\delta_l$) between the SC-link's section element (i.e., T- and L-plates), which can be estimated by applying the following relation:

$$\boldsymbol{\delta_l \cong \theta_P(h_d - t_f)} \qquad (2)$$

where $\theta_P$ represents the rotation between the link and the beam, and it is related to the geometrical properties of the frame according to the equation provided in Figure 2(a). Finally, the flag-shaped cyclic loop of the SC-link is shown in Figure 2(d) in terms of longitudinal shear force and longitudinal sliding ($F_l$ vs $\delta_l$). The longitudinal shear forces defining the entire cycle depend on three primary parameters: $F_{PT,0}$, $F_{FD}$ and $\Delta F_{PT}$. $F_{PT,0}$ is the initial post-tensioning force applied to the PT-bars; $F_{FD}$ is the sliding force developed at the friction interfaces; $\Delta F_{PT}$ is the increase of axial force in the PT-bars due to their elongation during the SC-link rotation and can be calculated as follows:

$$\boldsymbol{\Delta F_{PT} = K_{eq}\delta_l} \qquad (3)$$

where $\mu$ is the friction coefficient of the friction interfaces; $n_s$ and $n_b$ are, respectively, the number of friction surfaces and bolts employed in the FDs; $K_{eq}$ is the equivalent axial stiffness of the self-centring system, composed of PT-bars and disk springs defined as [21]:

$$\boldsymbol{K_{eq} = \frac{K_{PT}K_{ds}}{K_{PT}+K_{ds}};\ K_{PT} = \frac{n_{PT}E_{PT}A_{PT}}{l_{PT}};\ K_{ds} = \frac{n_{ds,par}}{n_{ds,ser}}K_{ds,1};} \qquad (4)$$

By referring to the $F_l$ vs $\delta_l$ behaviour (Figure *2*(d)), from a design point of view, the self-centring capability of the device is achieved if the initial post-tension in the PT-bars is higher than the slippage force acting in the FDs. Specifically:

$$\boldsymbol{F_4 \geq 0 \rightarrow F_{PT,0} \geq F_{FD}} \qquad (5)$$

The interested reader can refer to Lettieri *et al*. [21] for additional details on the behaviour of the proposed SC-link.

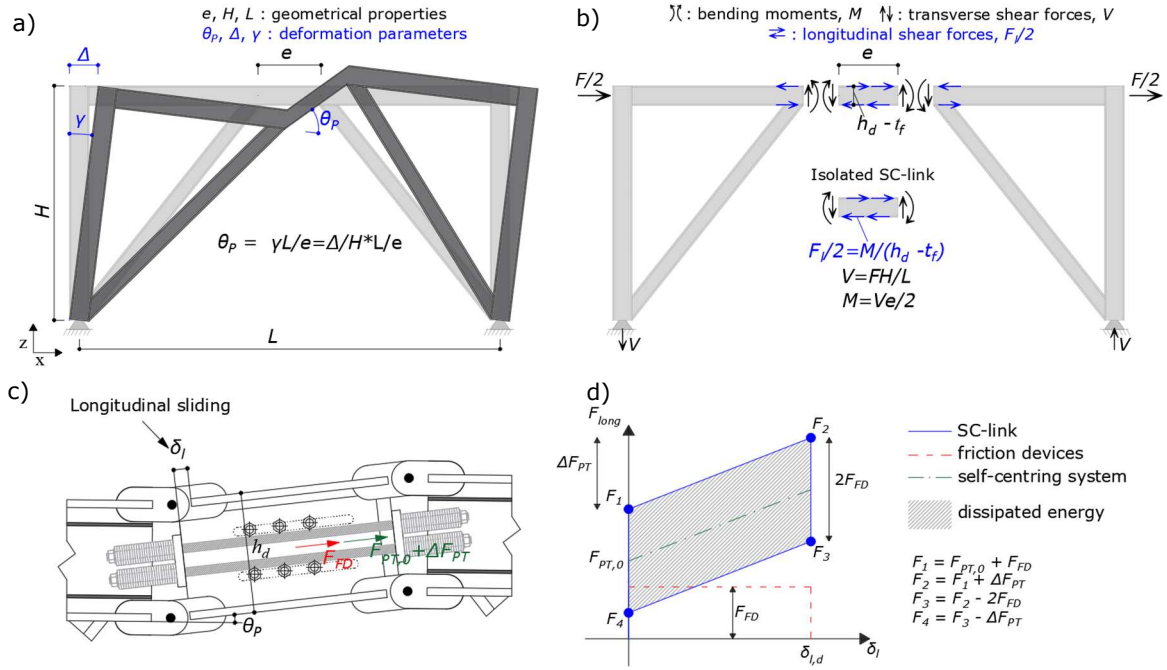


**Figure 2** (a) Deformed shape of the EBF; (b) free body diagram of the EBF; (c) deformed configuration of the SC-link and internal forces; (d) longitudinal shear force vs longitudinal sliding relationship.

## 2.2 Design procedure

The design of the SC-link is based on the structural analysis of the 'equivalent' conventional EBF system at the design limit state (i.e., Ultimate Limit State – ULS). The device is defined by proportioning *(i)* self-centring system, which is composed of PT-bars, anchor plates and disk springs; *(ii)* FDs; *(iii)* SC-link section properties (T- and L-plate geometry); *(iv)* pin connections. According to the analytical model presented in the previous section, the design actions are derived from Eqn. (1) considering $F$ as the equivalent lateral force to the seismic design action. Moreover, the design longitudinal sliding ($\delta_{l,d}$) is derived from Eqn. (2) considering $\theta_P$ as the design link rotation.

The self-centring capability is provided by distributing the design longitudinal shear force ($F_l$) between the FDs and the self-centring system, according to Eqn. (5). The design longitudinal shear force of the self-centring system is the initial post-tensioning force of the PT-bars (i.e., $F_{PT,0}$) and allows designing the number and dimension of the PT-bars. Successively, the number of disk springs in parallel and in series is calculated according to the following relationships:

$$\boldsymbol{n_{ds,par}} \geq \frac{N_{y,PT}}{F_{ds,1}} \qquad (6)$$

$$\boldsymbol{n_{ds,ser}} \geq \boldsymbol{n_{ds,par}} \boldsymbol{K_{ds,1}} \left( \frac{K_{PT} - K_{eq,1}}{K_{eq,1} K_{PT}} \right); \; \boldsymbol{K_{eq,1}} = \frac{N_{y,PT} N_{PT,0}}{\delta_{l,d}} \qquad (7)$$

where $N_{y,PT}$ is the yield strength of the PT-bar; $F_{ds,1}$ is the resistance capacity of a single disk spring; $N_{PT,0}$ is the post-tensioning force of the PT-bar. Successively, the anchor plates for the PT-bars are designed to have sufficient stiffness, guaranteeing the complete transmission of the restoring forces to the SC-link.

The FDs are designed such that the slippage force ($F_{FD}$) on the FD interfaces resists the remaining design longitudinal shear force. The number of bolts can be designed based on the Eqn. (3) by choosing the diameter and the class of the bolts, and ensuring that the pre-loading force in each bolt ($F_{pre\text{-}load,FD}$) is smaller than the maximum pre-loading force ($F_{p,Cd}$) defined in the Eurocode 3 [26].

The pin connections of the T- and L-plates should be designed to remain elastic and thus verified against $F_2$, $V_2$ and $M_2$ (maximum longitudinal shear force, maximum transverse shear and maximum bending moment, respectively). Furthermore, to allow the gap-opening mechanism of the SC-link, the T-plate's holes are designed to accommodate $\delta_{l,d}$. The pin connections are designed to transmit the transverse shear forces and bending moments according to Eurocode 3 requirements [26]. Additional details on the design procedure are provided in Lettieri *et al.* [21].

## 3 Experimental campaign

A SC-link has been designed following the design procedure described in Section 2 and tested under cyclic loading. The specimen includes the SC-link connected to a portion of the external beams through pin connections (Figure 3(a)). The plates constituting the T-, L-plates, the external beams and the pin connections are welded by complete-joint-penetration (CJP) groove welds. S355 is adopted for all components.

The self-centring system is realised employing two threaded high-strength M20 PT bars of 10.9 class, and the disk springs system consists of Belleville Disk Springs DIN 6796 arranged with one disk in parallel and 26 disks in series. FDs employ four M10 bolts of 10.9 class and friction interfaces with a friction coefficient of 0.53 based on previous experimental studies [27]. The initial post-tensioning axial force ($F_{PT,0}$) applied to the self-centring system is equal to 80 kN, while the bolt pre-loading force in the FDs provides a frictional sliding force ($F_{FD}$) equal to 35 kN. It is noteworthy that the aforementioned forces act as longitudinal shear forces. The corresponding transversal shear forces can be derived by applying Eqn. (1) and are respectively equal to 28 kN and 18 kN for $F_{PT,0}$ and $F_{FD}$.

The test setup is shown in Figure 3(a). The SC-link specimen was bolted into the setup between the loading system and the foundation. The actuator's centroid passed through the link's mid-span, ensuring the application of equal and opposite bending moments at the SC-link's ends. Linear variable differential transformers (LVDTs) were used to measure the deformation of the specimen. At the same time, strain gauges were employed to monitor the strains in the external beams and the axial load of the PT-bars. Cyclic loading was applied to the SC-link using the standardised protocol specified in the AISC provision [22] for testing EBF link-to-column connections. Figure 3(b) reports the test results regarding transverse shear (*V*) applied and lateral displacement.

## 4 Numerical simulations

### 4.1 Local behaviour

3D FE models of the specimen have been developed in ABAQUS [23] (Figure 3(c)). The FE model includes only the SC-link specimen, and eight-node linear brick elements (C3D8R) are used in the modelling. A 'tie constraint' simulates welding among the plated employed into the pin connections. The 'surface-to-surface' interaction property defines the FDs' contact behaviour among friction interfaces. The 'bolt load' is used to model the pre-loading in the bolts. In contrast, post-tensioning in the PT-bars is modelled by applying a 'predefined field temperature'. Additional modelling details can be found in Lettieri *et al.* [21].

Cyclic simulation has been performed and validated against the experimental results (Figure 3(b)). Additionally, the analytical cyclic response obtained based on the relationship described in Section 2.1 is reported in Figure 3(b). The comparison between the experimental, numerical, and analytical results shows a good correlation, denoting an accurate representation of the SC-link's behaviour in the numerical simulations. The experimental and numerical results for large displacement show an increase in the force predicted due to second-order effects not included in the analytical model. Finally, the Von Mises stress distribution is reported in Figure 3(d) for a SC-link displacement equal to 30 mm. The stress distributions confirm the investigated detail's low-yielding behaviour, highlighting only the minor yielding of some components (pin connections in Figure 3(d)).

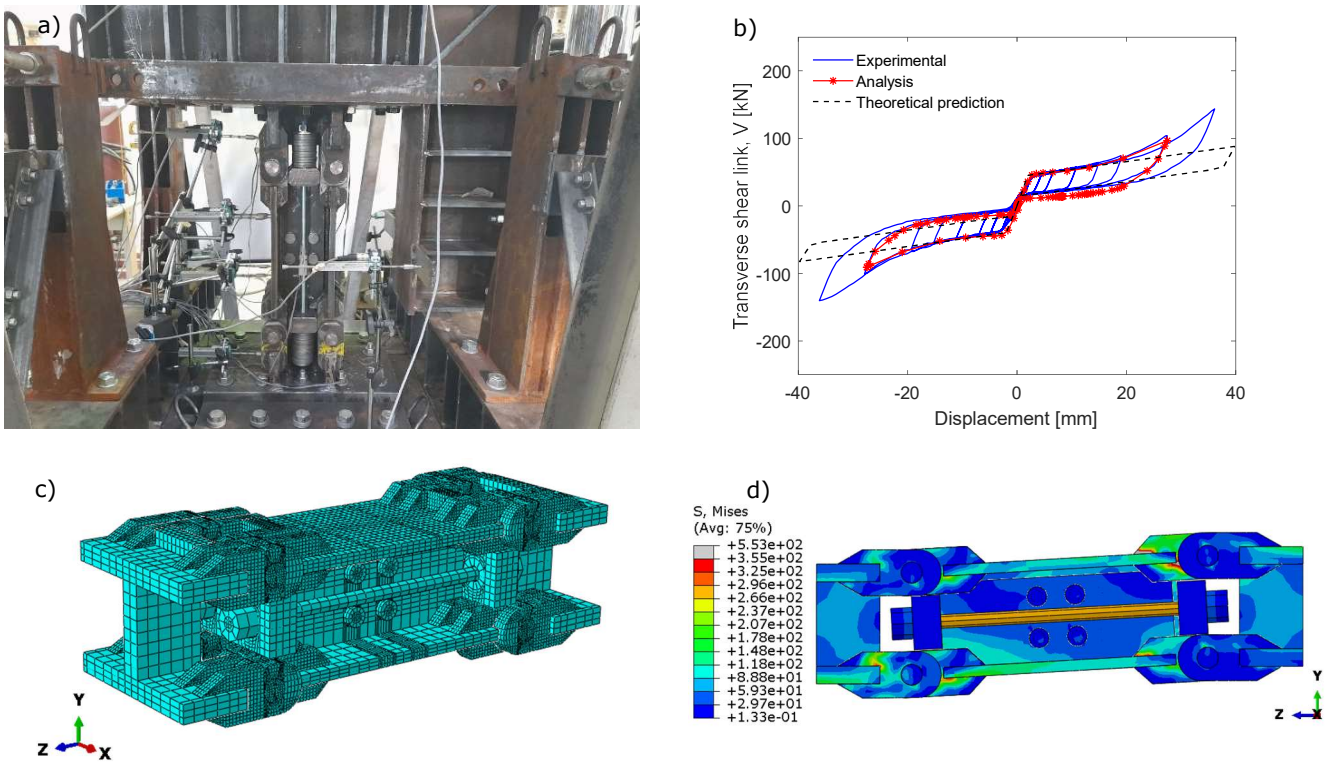


**Figure 3** (a) Experimental setup and instrumentation; (b) test results in terms of transverse shear (V) vs displacement; (c) overview of the 3D ABAQUS model; (d) Von mises stress distribution corresponding to a displacement of 30 mm.

### 4.2 Global response

A six-storey EBF has been designed according to Eurocode 8 with conventional links and successively upgraded with SC-links. The considered EBF is the lateral resisting system of a building whose geometrical properties are shown in Figure 4. The EBF with conventional links is designed considering a uniform permanent load $G_k$ = 4.5 kN/m$^2$, a uniform variable load $q_k$ = 2.0 kN/m$^2$ and claddings weighing 2.0 kN/m. A Type-1 elastic response spectrum with a peak ground acceleration equal to 0.35g and soil type C has been considered to define the seismic design actions at ULS [1]. The behaviour factor is assumed to equal 6 according to Eurocode 8 for EBF in DCH [1]. The lengths *e* of the links are limited at an upper value of 1.6 $M_{p,link}/V_{p,link}$ according to the provisions for short links. Steel S275 is employed for all structural elements (i.e., columns, beams, and braces). The design results for the conventional EBF are reported in Figure 4.

The SC-links employed in the upgraded configuration have been designed according to the procedure presented in Section 2.2. According to Eqn (5), the design actions are equal to 0.6*Fl* and 0.4*Fl* for the self-centring system and

FDs, respectively. A design link rotation equal to 0.08 rad is assumed, and Eqn. (2) provides the corresponding longitudinal sliding. The $F_2/F_1$ ratio (Figure 2(d)) is limited to 1.5 according to the link overstrength ($\Omega$) defined for short conventional links in [1]. Friction pads are chosen according to previous experimental tests by Cavallaro *et al.* [27] with a friction coefficient equal to 0.53. HV bolts of 10.9 class have been selected for the FDs, and high-strength bars of 10.9 class have been used for the self-centring system. Disk springs are finally arranged in series and parallel according to Eqns. (6)-(7).

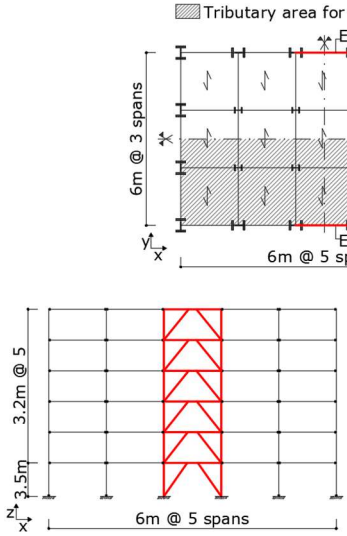


| Link/beam | Column | Bracing |
|---|---|---|
| HE 180 B | HE 280 B | HE 180 M |
| HE 280 B | HE 280 B | HE 200 M |
| HE 340 B | HE 300 B | HE 220 M |
| HE 360 B | HE 320 B | HE 220 M |
| HE 400 B | HE 400 B | HE 240 M |
| HE 450 B | HE 500 B | HE 240 M |

**Figure 4** Plan and elevation view of the case-study buildings.

The seismic performance of the EBF and SC-EBF is evaluated and compared. 2D FE models of the systems have been developed in OpenSees according to the modelling approach described in Lettieri *et al.* [21]. The structures are characterised by the same fundamental period of vibration of 0.79 sec. The corresponding first-mode spectral acceleration at the ULS is equal to 0.90g. The seismic responses have been evaluated through IDAs. A set of 30 natural ground motion records selected using REXEL [29] is used, and peak and residual interstorey drifts ($\theta_{max\text{-}peak}$ and $\theta_{max\text{-}res}$) are monitored during the analysis. The spectral acceleration corresponding to the first vibration mode ($S_a(T_1)$) is assumed as Intensity Measure (*IM*) and reported as the ratio between the IM value and the corresponding spectral acceleration at the ULS, $S_a(T_1)_{ULS}$. The threshold values of the residual drifts for DS1 and DS2 suggested by the FEMA P-58 [6], corresponding respectively to $\theta_{res\text{-}DS1}$ = 0.2% and $\theta_{res\text{-}DS2}$ = 0.5%, are considered to evaluate the self-centring capability of the structures. Figure 5 shows the IDA [28] results in terms of peak and residual quantities (Figure 5(a) and (b), respectively). It is possible to observe that the SC-EBF configuration experiences higher values of $\theta_{max\text{-}peak}$ (Figure 5(a)) than the traditional structure (EBF), denoting an increase in the frame's response at peak. Conversely, Figure 5(b) demonstrates that introducing SC-links in the SC-EBF allows a significant reduction of residual deformations, ensuring the repairability of the structure without the need for realignment.

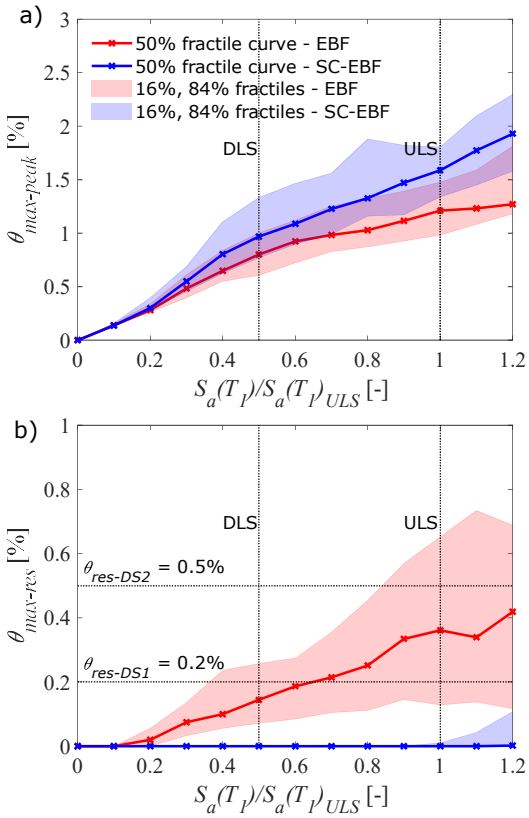


**Figure 5** IDAs comparison in terms of (a) peak and (b) residual interstorey drift.

## 5 Conclusions

This paper presents the experimental characterisation of the damage-free self-centring link's cyclic response recently proposed by the authors. The proposed device is tested under cyclic loading according to the AISC standardised protocol. Numerical simulations have been performed in ABAQUS and validated against test results. Aiming to capture the main effects of the proposed device's introduction on the seismic performance of Eccentrically Braced Frames, a six-storey case-study structure is designed according to Eurocode 8 and successively upgraded with damage-free self-centring links. The seismic performance of the systems has been investigated and compared by performing Incremental Dynamic Analyses on simplified two-dimensional models in OpenSees. The experimental tests demonstrated the potential of the innovative device to be used in seismic resilient Eccentrically Braced Frames since it can avoid residual deformations. The numerical results show that the introduction of the proposed and investigated connection increases the seismic response of the structures at peak and eliminates residual deformations.

## Acknowledgements

This research was partially supported by the Royal Society – International Exchange programme under the grant agreement IES\R3\213175. Any opinions, findings, conclusions or recommendations expressed in this paper are those of the authors and do not necessarily reflect the views of the Royal Society.

## References

[1] EN 1998-1 (2004) *Eurocode 8: Design of structures for earthquake resistance – Part 1: General rules, seismic actions and rules*

*for buildings*. European Committee for Standardization, Brussels.

[2] Freddi F., Novelli V., Gentile R., Veliu E., Andonov A., Andreev S., Greco F., Zhuleku E. (2021) *Observations from the 26th November 2019 Albania Earthquake: the Earthquake Engineering Field Investigation Team (EEFIT) mission*, Bulletin of Earthquake Engineering, 19(5): 2013-2044.

[3] Stratan A., Dubina D. (2004) *Bolted links for eccentrically braced steel frames*. Proceedings of the fifth AIS/ECCS International Workshop Connections in Steel Structures V. behaviour, Strength and Design, Delft university of Technology, Netherlands, June 3-5.

[4] Mansour N., Christopoulos C., Tremblay R. (2011) *Experimental validation of replaceable shear link for eccentrically braced frames*. Journal of Structural Engineering, 137(10), 1141-1152.

[5] Bozkurt M.B., Asad S.K., Topkaya C. (2019) *Development of detachable links for eccentrically braced frames*. Earthquake Engineering & Structural Dynamics, 48, 1134-1155.

[6] FEMA P58-1 (2012). *Seismic Performance Assessment of Buildings. Volume 1 – methodology*. Applied Technology Council.

[7] McCormick, J., Aburano, H., Nakashima, M. (2008) *Permissible residual deformation levels for building structures considering both safety and human elements.* 14th World Conference on Earthquake Engineering (WCEE), October 12-17, Beijing, China.

[8] Latour, M., Rizzano, G., Santiago, A., Da Silva, L. (2019) *Experimental response of a low-yielding, self-centering, rocking CB joint with friction dampers*. Soil Dynamics and Earthquake Engineering; 116: 580–592.

[9] Freddi, F., Dimopoulos, CA., Karavasilis, TL. (2020) *Experimental evaluation of a rocking damage-free steel CB with friction devices*. Journal of Structural Engineering. (ASCE); 146(10): 04020217. DOI: 10.1061/(ASCE)ST.1943-541X.0002779.

[10] Elettore, E., Freddi, F., Latour, M., Rizzano, G. (2021) *Design and analysis of a seismic resilient steel moment resisting frame equipped with damage free self-centring column bases*. Journal of Constructional Steel Research, 179, 106543.

[11] Elettore E., Lettieri A., Freddi F., Latour M., Rizzano G. (2021) *Performance-Based Assessment of Seismic-Resilient Steel Moment Resisting Frames Equipped with Innovative Column Bases Connections*. Structures, 32, 1646-1664.

[12] Lettieri E., Elettore E., Pieroni L., Freddi F., Latour M., Rizzano G. (2022) *Parametric analysis of steel MRFs with self-centring column bases*. Steel Construction, 15(2), 91-99.

[13] Pieroni, L., Elettore, E., Freddi, F., Latour, M. (2021) *Optimised strategies for mid-rise seismic-resilient self-centring steel moment resisting frames.* The 9th European Conference on Steel and Composite Structures (Eurosteel 2020), Sheffield, UK, 1–3 September 2021.

[14] Dubina D., Stratan A., Dinu F. (2008) *Dual high-strength steel eccentrically braced frames with removable links*. Earthquake Engineering & Structural Dynamics, 37, 1703-1720.

[15] Cheng C.T., Hsu C.H. (2012) *Seismic behaviour of self-centring designed eccentrically braced frames*. 15th World Conference on Earthquake Engineering, Lisboa.

[16] Tong L., Zhang Y., Zhou X., Keivan A., Li R. (2019) *Experimental and Analytical Investigation of D-Type Self-Centering steel eccentrically braced frames with replaceable hysteretic damping devices*. Journal of Structural Engineering, 145(1).

[17] Al-Janabi Q., Yang T.Y. (2021) *Performance assessment of novel self-centring friction-based eccentrically braced frames*. Engineering Structures, 241, 112456.

[18] Xu X., Zhang Y., Luo Y. (2016) *Self-centering eccentrically braced frames using shape memory alloy bolts and post-tensioned tendons*. Journal of Constructional Steel Research, 125, 190-204.

[19] Askariani S.S., Garivani S., Hajirasouliha I., Soleimanian N. (2022) *Innovative self-centring systems using shape memory alloy bolts and energy dissipating devices*. Journal of Constructional Steel Research, 190, 107-127.

[20] Mirzai N.M., Attarnejad R., Hu J.W. (2021) *Experimental investigation of smart shear dampers with re-centring and friction devices*. Journal of Building Engineering, 35, 102018.

[21] Lettieri A., de la Pena A., Freddi F., Latour M. (2023) *Damage-free self-centring link for eccentrically braced frames: development and numerical study*. Journal of Constructional Steel Research, Special Issue on 'Seismic Resilient Steel Structures', 201, 107727.

[22] ANSI/AISC 341-16 (2016). *Seismic provisions for structural steel buildings*. American Institute of Steel Construction, Chicago, USA.

[23] ABAQUS – Analysis User's Manual Version 6.17, Abaqus Inc., 2017.

[24] Mazzoni S., McKenna F., Scott M.H., Fenves G.L. (2009) *OpenSEES: Open System for Earthquake Engineering Simulation*. Pacific Earthquake Engineering Research Centre (PEER), University of California, Berkeley, CA.

[25] Kasai K., Han X. (1997) *New EBF design method and applications: Redesign and analysis of US-Japan EBF*. 2nd International Conference on Behaviour of Steel Structures in Seismic Areas (STESSA).

[26] EN 1993-1-8 (2005), *Eurocode 3: Design of steel structures, Part 1-8: Design of steel structure: General rules and rules for buildings*. European Committee for Standardization, Brussels.

[27] Cavallaro, GF., Francavilla, A., Latour, M., Piluso, V., Rizzano, G. (2008) *Cyclic behaviour of friction materials for low yielding connections*. Soil Dynamics and Earthquake Engineering; 114: 404–423.

[28] Vamvatsikos D., Cornell C.A. (2002) *Incremental Dynamic Analysis*. Earthquake Engineering Structural Dynamics, 31(3), 491-514.

[29] Iervolino I., Galasso C., Cosenza E. (2010). *REXEL: Computer aided record selection for code-based seismic structural analysis*, Bulletin of Earthquake Engineering, 8, 339-362.